Optical reading of multistate non-volatile oxide memories based on the switchable ferroelectric photovoltaic effect

A Zing, S Matzen, K Rani, T Maroutian, G Agnus, P Lecoeur

Optical reading of multistate non-volatile oxide memories based on the switchable ferroelectric photovoltaic effect

A. Zing[1], S. Matzen[1], K. Rani[1], T. Maroutian[1], G. Agnus[1], P. Lecoeur[1]*

[1] Université Paris-Saclay, CNRS, Centre de Nanosciences et de Nanotechnologies (C2N), 10 Boulevard Thomas Gobert, 91120 Palaiseau, France

* corresponding author: sylvia.matzen@universite-paris-saclay.fr

Abstract

Intensive research into functional oxides has been triggered by the quest for a solid-state universal memory with high-storage density, non-volatility, high read/write speed, and random access. The ferroelectric random-access memory (FeRAM), in which the information is stored in the spontaneous ferroelectric polarization of the material, offers great promise as non-volatile and multistate memory, but its destructive electrical reading step requires a rewrite step after each reading, increasing energy consumption. As an alternative, optical non-destructive read-out is based on the ferroelectric polarization dependence of the photovoltaic response in materials, and has been reported in two-states ferroelectric memories and multistate devices with limited photocurrent switchability due to asymmetric interfacial effects. In this work, we report a non-volatile oxide memory device based on a symmetric heterostructure with eight stable and well-controlled remanent polarization (P_r) states, written electrically by voltage pulse and read optically through polarization-dependent short-circuit photocurrent I_{sc} or open circuit photovoltage V_{oc}. This symmetric capacitor demonstrates a clear proportionality between J_{sc} (V_{oc}) and P_r, allowing to achieve a 100 % switchability of the photovoltaic response. The memory devices based on 3-bit data storage show good performance in terms of data retention, fatigue behavior, and repeatability of writing and reading cycles. Thanks to the very high sensitivity of the optical reading method, the number of states could largely exceed eight, being limited only by the electrical writing step precision. These results are particularly exciting for the development of next-generation ferroelectric memory devices with increased memory storage density and lower power consumption.

The pursuit of a solid-state universal memory with high storage density, non-volatility, high read/write speed, and random access has sparked intense study into functional oxides. Among memory devices, the ferroelectric random-access memory (FeRAM) offers great promise because it is non-volatile and the read/write process can be completed within nanoseconds [1-4]. In a FeRAM, the information is stored in the spontaneous ferroelectric polarization of the material, showing two stable directions which represent '0' and '1'. A writing external voltage pulse is applied to switch the polarization between both states and a reading voltage pulse is used to detect the current during polarization switching and assess the polarization direction. Since there are increasing demands for computational density and functionalities for next-generation electronics, the possibility to create multistate polarization by overcoming the bistability of ferroelectrics appears thus particularly exciting. In ferroelectric layers integrated into capacitor structures, creating multiple stable states with distinct polarization values during the writing step was demonstrated by engineering switching pathways [5], or by adjusting the displacement current [6]. In this work, eight stable and reproducible polarization states (i.e., 3-bit data storage) were reported, allowing to triple or quadruple the memory density, even at existing feature scales [6]. However, while ferroelectric memories allow enhanced storage density, their development is hampered by the destructive reading step and thus the need to rewrite the polarization state after each reading, increasing energy consumption. In addition, enough current must be generated during the ferroelectric switching to sense the information

state, limiting the device lateral downscaling. Developing non-destructive read-out methods of multistate ferroelectric memories appear thus particularly crucial for FeRAM to be competitive in the memory market.

In this context, taking advantage of the photovoltaic effect in ferroelectrics appears particularly interesting for developing an optical reading method of the polarisation states. Thanks to their non-centrosymmetry, ferroelectric materials exhibit indeed the bulk photovoltaic effect [7-10], which is the spontaneous generation of photocurrent and photovoltage within the material under illumination with photon energy above the bandgap. Unlike the classical photovoltaic (PV) effect in semiconductors, which requires a driving electric field, usually created at p-n junctions, for the separation of the photocarriers, the electron-hole pairs are efficiently separated in a ferroelectric material through the existence of its polarization. The direction of the ferroelectric polarization can control the sign of both short-circuit photocurrent (I_{sc}) and open-circuit voltage (V_{oc}), theoretically allowing for 100% switchability of the PV characteristics. This polarization-dependence of the PV properties has been reported in many studies, from bulk ferroelectrics [11, 12] to thin films [13-20]. As the signs of both I_{sc} and V_{oc} depend on the polarization direction, they can serve as read-out signals in a memory device. This optical reading method is non-destructive, so it does not require to apply voltage to restore the original polarization state. This would double the endurance of FeRAM, simplify the storage operation, and reduce power consumption. The feasibility of this method has been first demonstrated in 2013 with a non-volatile memory device based on $BiFeO_3$ ferroelectric thin film [17]. Both V_{oc} and I_{sc} were reversed with the ferroelectric polarization and the data retention, fatigue performance, and energy consumption of the devices compared favorably with other non-volatile memories. This approach to create a non-volatile memory technology based on the polarization-dependent PV effects in ferroelectrics has been extended to resistive switching memories [21-23], including ferroelectric tunnel junctions [24]. The non-destructive optical reading of polarization states offers thus great promise for next-generation ferroelectric multistate memory devices. Very recently, a control of I_{sc} has been reported by modulating the pulse voltage in a ferroelectric thin film combined with a dielectric layer [25]. A proof-of-concept of ferroelectric photovoltaic synapses was proposed in 2021 that uses polarization-controlled photocurrent as the readout in polycrystalline PZT thin film [26]. Both studies are exciting for the development of pulse-controlled nonvolatile multilevel memory devices with non-destructive optical reading. In these devices, however, the photocurrent was not 100% switchable with the ferroelectric polarization due to an asymmetric behavior originating from interfacial PV effects and the presence of an unswitchable internal bias field.

In this work, we report a multistate non-volatile oxide memory device with non-destructive optical reading, based on a symmetric heterostructure allowing achieving a 100 % switchability of the PV properties with the ferroelectric polarization. The device demonstrates multiple well-controlled remanent polarization (P_r) states written electrically by voltage pulse and read optically through polarization-dependent I_{sc} and V_{oc}. Thanks to the very high sensitivity of the optical reading method, the number of states in the memory device is found to only depend on the precision of the electrical writing step. For all written polarization states, the non-volatility and endurance performance under writing and reading cycles have been measured.

Epitaxial ferroelectric thin films (120 nm-thick) of tetragonal PZT ($Pb(Zr_{0.2},Ti_{0.8})O_3$) have been integrated into symmetric capacitor geometry with $SrRuO_3$ (SRO) bottom and top electrode. The layers have been grown by pulsed laser deposition (details in supplemental material) on $SrTiO_3$(001) substrate (STO). The oxide heterostructure presents high crystalline quality and smooth surface, as evidenced by x-ray diffraction and atomic force microscopy (figure S1).

Capacitor structures of different lateral sizes from 10 µm to 50 µm were defined by optical lithography and Ion Beam Etching of the top SRO electrodes. The latter were electrically connected to larger Pt electrodes, insulated from the PZT layer by a SiN layer (Figure 1(a)). The ferroelectric response of the devices was studied using a TF Analyzer 1000 AixACCT in Positive-Up Negative-Down (PUND) mode, using triangular pulses with 2 ms width. Photovoltaic measurements (I(V), $I_{sc}(t)$, and $V_{oc}(t)$) were performed using Keithley 2635 under UV illumination from the top, at 365 nm wavelength, corresponding to photon energy above the bandgap of PZT [20]. The UV illumination was provided by a diode with an incident fluence of 35 mW/cm². Note that the 120 nm thickness of the ferroelectric layer was chosen to be quite close to the UV photons penetration depth, while ensuring good electrical properties with limited leakage current over the tens of microns wide capacitors. For all electrical measurements the voltage bias was applied between the top electrode of each device and the grounded bottom electrode.

In the initial state, the capacitors present an imprinted ferroelectric loop, probably caused by charged defects trapped at the FE/electrode top interface. Indeed, capacitors of SRO/PZT/Pt fabricated from epitaxial PZT films grown on STO/SRO with the same conditions do not show such imprint [20]. To reach optimal operation of the devices, 10^8 cycles of bipolar switching were applied with an amplitude of 2.2V. The effect of this initial cycling on the device properties (P_r, J_{sc}, V_{oc} and switchability) is detailed in Supplemental Material (Figure S2). This procedure allows to get robust and symmetric FE and PV properties and has been applied to all devices in this work.

The device has well defined up and down P_r states of +65 and -65 µC/cm² and coercive voltage of +1V and -1V (PUND loop in Figure 1(b)). I_{sc} and V_{oc} measured from I-V characteristics (Figure 1(c)) are found to strongly depend on the polarization states. The I_{sc} and V_{oc} values are 1.99 nA and -0.82 V in the up state, and they switch signs to -2.75 nA and 1.07 V in the down state. This polarization dependence of the PV properties is expected by considering either the bulk PV mechanism or the depolarizing field as the driving force of the PV effect in the FE layer. Note that our symmetric SRO/PZT/SRO capacitors reach very high photocurrent S_I and photovoltage S_V switchability (above 85%), as further described below.

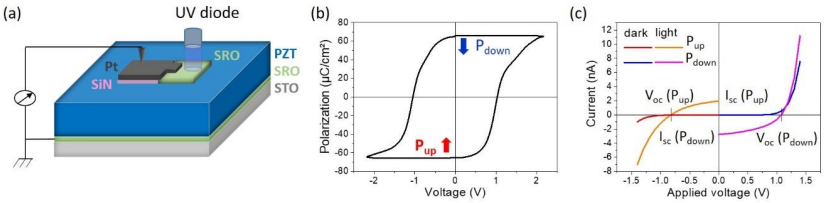

Figure 1: (a) Sketch of the device and setup for the ferroelectric and photovoltaic measurements. (b) Ferroelectric hysteresis loop measured by PUND of a typical capacitor (50 µm size). (c) Current Vs voltage measurement both in the dark and under UV illumination for up and down poling states (after -2.2V and +2.2V poling).

As expected, the PV response of the device depends on the light intensity. While I_{sc} increases linearly as a function of the diode power, V_{oc} gets saturated from an incident fluence above 20 mW/cm² (Figure S3). The device exhibits typically saturated V_{oc} of 1V and J_{sc} of 20 µA/cm² at 20 mW/cm² corresponding to a photocurrent responsivity of 1 mA/W. This is higher than the PV response observed in $BiFeO_3$ memory devices under the same incident fluence (≈ 3 10^{-2} mA/W and $V_{oc} \approx 0.2$ V, [17]), indicating that the PV mechanism in our system is more efficient.

Among previous results published for PZT thin films, very few report J_{sc} and V_{oc} measurements under UV illumination with a defined fluence. In ref. [15], switchable J_{sc} was measured with 1 mA/W responsivity but no V_{oc} report, while in ref. [27] 2.7 mA/W responsivity and 0.71 V saturated V_{oc} were obtained but without switchability due to a strong interface asymmetry.

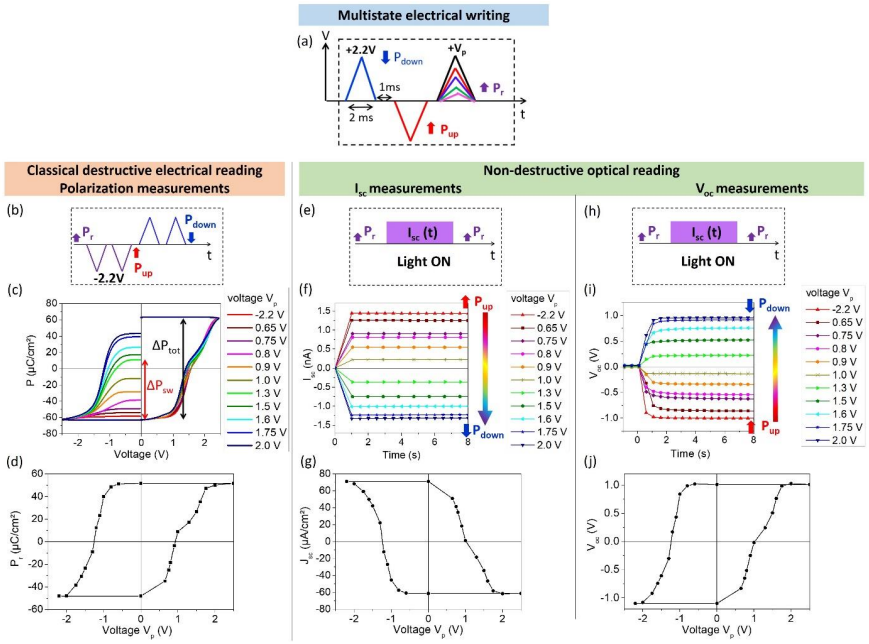

Figure 2 : (a) Writing voltage pulses sequence to define multiple particular P_r states by controlling the V_p values. (b-d) Usual method of destructive electrical reading: (b) reading voltage pulses, (c) measurements of polarization P used to extract the switched polarization ΔP_{sw} and deduce the P_r value for each writing state, and (d) resulting hysteresis loop of P_r as function of V_p. (e-j) Non-destructive optical reading of the P_r states (written by V_p voltage pulse) through the measurement of I_{sc} (e) and V_{oc} (h) under UV illumination in a typical capacitor (50 µm size). Measurements of I_{sc} (f) and V_{oc} (i) for each written state. Resulting hysteresis loops of short-circuit photocurrent density J_{sc} (g) and open-circuit voltage V_{oc} (j) as function of V_p (data from another device), showing that they can serve as read-out signals for the polarization state.

The method of electrical writing of multiple P_r states and their reading is described in Figure 2. After saturating the polarization in the up state (P_{up}), a voltage pulse (Figure 2(a)) of controlled amplitude V_p is applied to define particular P_r values. This information can be read following the classical destructive electrical reading method (Figure 2(b-d)). In this method, negative electrical pulses (of -2.2 V, Figure 2(b)) are used to switch P_r to P_{up}, allowing measuring the amount of polarization switched to reach the up state (ΔP_{sw}). Positive electrical pulses are further applied to switch the polarization from P_{up} to P_{down} and assess the total amount of switchable polarization (ΔP_{tot}). Each pulse is repeated twice (similar to the PUND mode) in order to remove any non-ferroelectric contribution to the measured polarization. The measured polarizations following this reading pulse sequence are shown in Figure 2(c) for each initial state written by V_p and allow to extract each P_r value using the equation: $P_r = \Delta P_{tot}/2 - \Delta P_{sw}$. This electrical reading method provides thus access to the stored polarization value P_r, which,

as expected, follows a hysteresis loop as function of the writing pulse amplitude V_p (Figure 2(d)) and evidences the capability to write multistate polarization in the memory device. The non-destructive optical reading method is presented in Figures 2(e-j). Measurements of I_{sc} and V_{oc} under UV illumination have been performed (Figures 2(f, i)) on the device for each written P_r state. Very stable photocurrent and photovoltage are observed whose values clearly reflect the polarization state. Both photocurrent and photovoltage follow a hysteresis loop as function of V_p (Figures 2(g, j)), very similar to the P_r loop (Figure 2(d)).

To investigate quantitatively the polarization-dependence of the PV response, J_{sc} and V_{oc} have been plotted as function of P_r (Figures 3(a, b)). Both J_{sc} and V_{oc} are clearly proportional to P_r. By considering the depolarizing field E_{dep} as the driving field for the photocurrent, following Ref. [20,28] J_{sc} can be expressed as $J_{sc} = -(\alpha\, \sigma_{pv} / \varepsilon)\, P_r$ with α the fraction of unscreened polarization, σ_{pv} the photoconductivity and ε the dielectric permittivity of the ferroelectric layer ($\varepsilon = \varepsilon_0\, \varepsilon_r$ with ε_0 the vacuum permittivity and ε_r the dielectric constant). Using this equation, a fraction of unscreened polarization α=3.5% is estimated from the slope of the J_{sc}-P_r dependence and the values of σ_{pv} ($5.52\ 10^{-8}$ S/m) and ε_r (211) measured for the device under illumination. This agrees with the expected order of magnitude for screening efficiency [28] and is consistent with the values previously reported for capacitors of $BaTiO_3$ ($\alpha \approx 3\%$ [18]) and PZT (α=1.5% [20]). The depolarizing voltage $V_{dep} = E_{dep}\, d$, with d the film thickness, can then be calculated for each P_r state as plotted in Figure 3(b). The experimental V_{oc} values are smaller than but quite close to V_{dep}, with photogenerated carriers cancelling almost completely the depolarizing field. This can thus be the origin of the measured PV response in the devices, even if the bulk PV mechanism cannot be ruled out. The measured proportionality between J_{sc} (V_{oc}) and P_r is the key to allow a 100% switchability of the PV response when switching the polarization from P_r to $-P_r$. In other reports [18, 20], the switchability was limited by the presence of an unswitchable internal electric field in the ferroelectric layer integrated between asymmetric electrodes, that translated into a cancelation of J_{sc} and V_{oc} for some non-zero P_r values. In this work, 100% switchability is achieved (S_V=98.4% and S_I=99.4%) which makes the optical reading of the polarization state much easier. As J_{sc} and V_{oc} are both proportional to P_r, the optical reading of the polarization state can be performed either by J_{sc} or V_{oc} measurements, with V_{oc} being independent on the device lateral size and less sensitive to the light power.

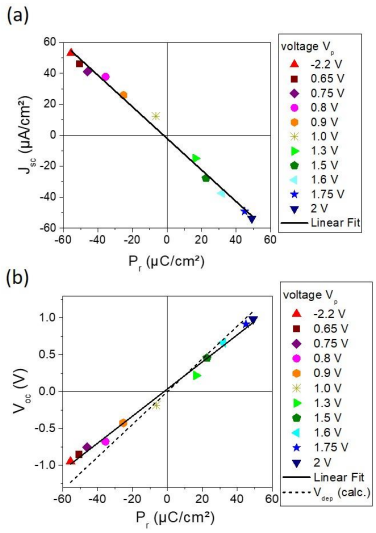

Figure 3: (a) J_{sc} and (b) V_{oc} as function of P_r written in several states (by V_p pulse), showing a linear relationship. V_{dep} calculated from the depolarizing field model.

For practical non-volatile memory applications, long data retention is required. This has been monitored by J_{sc} and V_{oc} measurements up to more than 3 months (Figures 4(a, b)). The P down state is observed to evolve slightly within the first 10 days after electrical writing. Otherwise, the information stored is quite stable over time. Note that the intermediate state with zero polarization shows even more remarkable stability, as observed previously by electrical reading in Ref. [29]. V_{oc} was also measured under light illumination (Figure 4(c)) for several polarization states, showing good retention. The devices fatigue behavior was further tested for optical reading cycles (Figures 4(d, e)) and electrical writing cycles (Figures 4(f, g)). Up to 10^6 ON-OFF illumination cycles were used to test repeating optical readings and no change was measured in V_{oc} and J_{sc}, confirming that the optical reading through J_{sc} and V_{oc} is non-destructive and reliable because light illumination does not affect the devices polarization state. Writing endurance test was performed by applying repeating bipolar electrical switching cycles of 2.2 V up to 10^8 cycles (Figure 4(f, g)). Once again, no deterioration of the J_{sc} and V_{oc} signals was measured under repeated cycles.

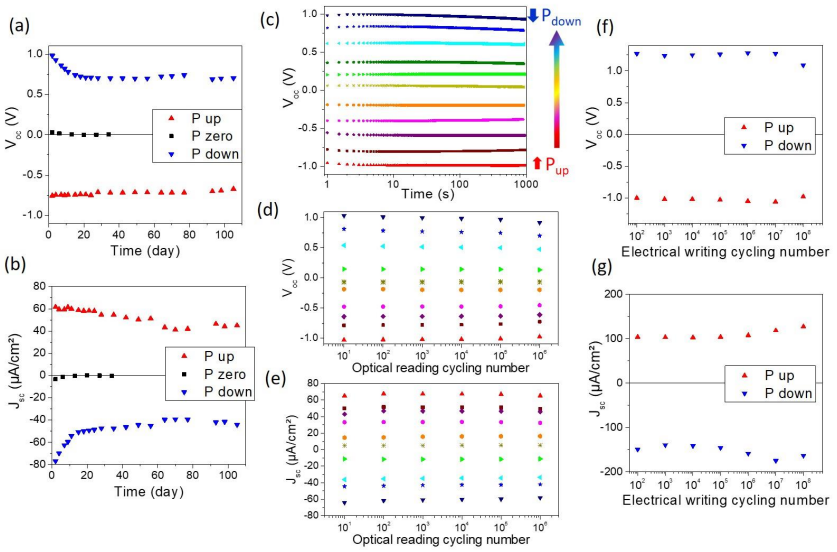

Figure 4: J_{sc} (a) and V_{oc} (b) as function of time for 3 states: up, down and intermediate ($P_r \approx 0$). (c) Retention under illumination of many polarization states read by V_{oc} measurements. Dependence of V_{oc} (d) and J_{sc} (e) as a function of the number of optical reading cycles for many polarization states. Dependence of V_{oc} (f) and J_{sc} (g) as a function of the number of electrical writing cycles for up and down polarization states for another 50 µm device.

To increase memory storage density, the multiple polarization states must be deterministically controlled. The same V_p writing pulses have been applied several times to the same device to test the repeatability of the writing procedure. The information states have been accessed by V_{oc} and J_{sc} measurements. Writing pulses performed on the same day (d0) show very small changes in the read-out signals for all P_r states (changes of less than 20 mV for V_{oc} and less than 2 µA/cm² for J_{sc}). The same writing procedure has been performed over 50 days. In Figures 5(a, b), the average of 6 measurements are shown with their standard deviation for each P_r state. The difference between d0 and over 50 days seems to indicate that the ferroelectric loop evolves slightly over time, so the same V_p pulse does not write the exact same P_r state anymore. While 11 P_r states have been written, some of them cannot be differentiated anymore. From this set of data, we can conclude that up to 8 polarization states (highlighted in Figure 5(a)) can be written electrically and distinguished without error by optical reading, allowing to increase the memory density, without reducing the lateral dimensions, to 3-bit data storage. By monitoring the electrical signal during the writing sequence, more polarization states could be defined and read optically. By adjusting the displacement current during the electrical writing pulse, Lee *et al* [6] have demonstrated that the polarization can be very precisely controlled in PZT thin films with a standard deviation of less than 1.5 µC/cm². Such changes in P_r will correspond to a change of 28 mV for V_{oc}. The V_{oc} reading method is thus very sensitive to small changes in polarization value, more sensitive than the classical electrical reading and does not limit the maximum number of stored information levels. We thus believe that much more than 8 states could be stored in a ferroelectric memory device and accessed by V_{oc} read-out signals. Finally, the V_{oc} read-out signal has been measured for several devices for both up and down polarization states (Figure 5(c)) and it shows the high yield and good uniformity of the memory devices.

The V_{oc} value is independent on the memory cell size, whereas the I_{sc} value scales with the size (Figure S4). So further increase in data storage could be achieved by downscaling the devices and using the V_{oc} optical reading method. In addition to the lateral downscaling, it would be also interesting to investigate the effect of ferroelectric thickness downscaling on the switchability of the PV response, in the objective of miniaturization and decrease of operating voltage.

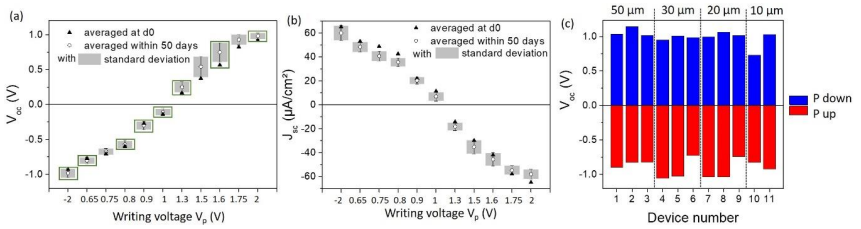

Figure 5: V_{oc} (a) and J_{sc} (b) read-out signals measured for each P_r state written several times electrically by V_p pulse. 8 polarization states (highlighted by green rectangles in (a)) can be reasonably stored in the memory device and distinguished by optical reading. (c) V_{oc} values for up and down P_r states in several devices of 50, 30, 20 and 10 μm size, showing the high uniformity of the read-out signal and its independence with the device size.

In conclusion, we report symmetric SRO/PZT/SRO capacitors showing an efficient photovoltaic mechanism with high photocurrent responsivity and 1 V open circuit voltage under UV illumination. A clear proportionality between J_{sc} (V_{oc}) and P_r is measured, allowing achieving a 100 % switchability of the PV response. Thanks to this quantitative polarization dependence of J_{sc} and V_{oc}, both can be used as a non-destructive read-out signal of the polarization states in ferroelectric memory devices. The V_{oc} optical reading method is found to be better-suited to developing memory cells with increased data storage and lower energy consumption. Multiple polarization states have been created, whose number is only limited by the electrical writing step precision thanks to the very high sensitivity of V_{oc} to the polarization. Oxide memory devices based on 3-bit data storage have been assessed, showing very good performance in terms of data retention, fatigue behavior, and repeatability of writing and reading cycles. This reported non-destructive optical reading of multistate polarization based on the switchable polarization-dependent PV effects in ferroelectrics offers great promise for next-generation ferroelectric memory devices with increased memory storage density and lower power consumption.

Acknowledgements
Research at the Center for Nanoscience and Nanotechnology was supported by the French RENATECH network and by the French National Research Agency (ANR) – Project UP-DOWN (Project No. ANR-18-CE09-0026-04). We thank Raphaël Haumont (ICMMO, Paris-Saclay University) for providing the PZT ceramic target for PLD deposition.

Data availability statement: The data that supports the findings of this study are available within the article [and its supplementary material].

Supplementary Material

See supplementary material for details about: a) growth parameters, crystal structure, and surface morphology; b) initial cycling procedure; c) dependence of the PV response with the light intensity; d) photocurrent reproducibility among the memory devices.

Authors contribution

A Zing, S Matzen, K. Rani, T Maroutian, G Agnus, P Lecoeur

The project idea was initially developed by S.M. and P. L. The growth of PZT thin films by PLD and their structural characterization (XRD) was done by K. R. and T. M. The patterning of the PZT into devices was done by S. M. The ferroelectric and photovoltaic measurements were performed by A. Z. with the help of K. R. and G. A. under the supervision of S. M. S.M. wrote the paper with significant contribution from A. Z. and T. M. All authors discussed the manuscript.

References

[1] S. S. Eaton, D. B. Butler, M. Parris, D. Wilson, and H. McNeille, IEEE Intern. Solid State Circuits Conf. Digest of Technical Papers 130 (1988).
[2] J. Evans and K. Womack, IEEE J. Solid-State Circuits 23, 1171 (1988).
[3] R. E. Jones, P.D. Maniar, R. Moazzami, P. Zurcher, J.Z. Witowski, Y.T. Lii, P. Chu, S.J. Gillespie, Thin Solid Films 270, 584 (1995).
[4] H. Ishiwara, Journal of Nanoscience and Nanotechnology 12, 7619 (2012).
[5] R. Xu, S. Liu, S. Saremi, R. Gao, J.J. Wang, Z. Hong, H. Lu, A. Ghosh, S. Pandya, E. Bonturim, Z.H. Chen, L.Q. Chen, A.M. Rappe and L.W. Martin, Nat. Comm. 10, 1282 (2019).
[6] D. Lee, S. M. Yang, T. H. Kim, B. C. Jeon, Y. S. Kim, J.-G. Yoon, H. N. Lee, S. H. Baek, C. B. Eom, and T. W. Noh, Adv. Mater. 24, 402 (2012).
[7] A. G. Chynoweth, Phys. Rev. 102, 705 (1956).
[8] V. M. Fridkin, A. A. Grekov, N. A. Kosonogov and T. R. Volk, Ferroelectrics 4, 169 (1972).
[9] A. M. Glass, D. von der Linde and T. J. Negran, Appl. Phys. Lett. 25, 233 (1974).
[10] C. Paillard, X. Bai, I. C. Infante, M. Guennou, G. Geneste, M. Alexe, J. Kreisel and B. Dkhil, Adv. Mater. 28, 5153 (2016).
[11] F. Micheron, Ferroelectrics 21, 607 (1978).
[12] L. Wu, A. M. Burger, A. L. Bennett-Jackson, J. E. Spanier and P. K. Davies, Adv. Electron. Mater. 7, 2100144 (2021).
[13] Y. S. Yang, S. J. Lee, S. Yi, B. G. Chae, S. H. Lee, H. J. Joo and M. S. Jang, Appl. Phys. Lett. 76, 774 (2000).
[14] K. Yao , B. K. Gan , M. Chen , S. Shannigrahi , Appl. Phys. Lett. 87, 212906 (2005).
[15] L. Pintilie, I. Vrejoiu, G. Le Rhun and M. Alexe, J. Appl. Phys. 101, 064109 (2007).
[16] D. Lee, S. H. Baek, T. H. Kim, J.-G. Yoon, C. M. Folkman, C. B. Eom, T. W. Noh, Phys. Rev. B 84, 125305 (2011).
[17] R. Guo, L. You, Y. Zhou, A. S. Lim, X. Zou, L. Chen, R. Ramesh, J. Wang, Nat. Commun. 4, 1990 (2013).
[18] F. Liu, I. Fina, D. Gutierrez, G. Radaelli, R. Bertacco and J. Fontcuberta, Adv. Electron. Mater. 1, 1500171 (2015).
[19] S. Cheng, Z. Fan, L. Zhao, H. Guo, D. Zheng, Z. Chen, M. Guo, Y. Jiang, S. Wu, Z. Zhang, J. Gao, X. Lu, G. Zhou, X. Gao and J.-M. Liu, J. Mater. Chem. C 7, 12482 (2019).
[20] K. Rani, S. Matzen, S. Gable, T. Maroutian, G. Agnus and P. Lecoeur, J. Phys.: Condens. Matter 34, 104003 (2022).
[21] Z. Lu, X. Yang, C. Jin, P. Li, J.-G. Wan, and J.-M. Liu, Adv. Electron. Mater. 4, 1700551 (2018).
[22] H. Gao, Y. Yang, Y. Wang, L. Chen, J. Wang, G. Yuan, and J.-M. Liu, ACS Appl. Mater. Interfaces 11, 35169 (2019)
[23] M. Wei, M. Liu, L. Yang, B. Xie, X. Li, X. Wang, X. Cheng, Y. Zhu, Z. Li, Y. Su, M. Li, Z. Hu, J.-M. Liu, Ceramics International 46, 5126 (2020).
[24] W. J. Hu, Z. Wang, W. Yu and T. Wu, Nat. Comm. 7, 10808 (2016).
[25] S.-J. Chang, S.-Y. Chen, P.-W. Chen, S.-J. Huang, and Y.-C. Tseng, ACS Appl. Mater. Interfaces 11, 33803 (2019).

[26] S. Cheng, Z. Fan, J. Rao, L. Hong, Q. Huang, R. Tao, Z. Hou, M. Qin, M. Zeng, X. Lu, G. Zhou, G. Yuan, X. Gao, J.-M. Liu, iScience 23, 101874 (2020).
[27] M. Qin, K. Yao, and Y. C. Liang, Appl. Phys. Lett. 93, 122904 (2008).
[28] R. R. Mehta, B. D. Silverman and J. T. Jacobs, J. Appl. Phys. 44, 3379 (1973).
[29] D. Zhao, I. Katsouras, K. Asadi, W. A. Groen, P. W. M. Blom, and D. M. de Leeuw, Appl. Phys. Lett. 108, 232907 (2016).